Larhyss Journal, ISSN 1112-3680, n°63, Sep 2025, pp. 215-232

ASSESSMENT OF ACTUAL EVAPOTRANSPIRATION AND WATER STRESS FROM LANDSAT ETM+ SATELLITE DATA USING THE PRIESTLEY–TAYLOR MODEL IN THE HABRA PLAIN, ALGERIA

HAMIMED A.*, BENSLIMANE M., KHALDI A., NEHAL L., ZAAGANE M.

Research on Biological Systems and Geomatics Laboratory, University of Mascara, P.O. Box 305, Mascara, 29000, Algeria

(*) hamimed@dr.com

Research Article – Available at http://larhyss.net/ojs/index.php/larhyss/index
Received November 12, 2024, Received in revised form August 17, 2025, Accepted August 19, 2025

ABSTRACT

In semi-arid regions such as the Habra Plain in northwestern Algeria, accurately estimating actual evapotranspiration (ET) is critical for effective agricultural water management. This study presents a remote sensing-based methodology integrating Landsat-7 ETM+ imagery with the Priestley–Taylor model to derive spatially distributed maps of actual evapotranspiration and water stress. The approach incorporates the "triangle method," which explores the relationship between land surface temperature (Ts) and the Normalized Difference Vegetation Index (NDVI), to parameterize the Priestley–Taylor coefficient (α) as a function of surface moisture conditions. Satellite-derived variables, including surface temperature, albedo, and vegetation indices, were corrected for atmospheric effects, while ground-based meteorological data informed the surface energy balance components.

Model validation was conducted through comparisons with ground-based Bowen ratio measurements and SEBAL model outputs, yielding a root mean square error (RMSE) of 49.6 W/m² and a correlation coefficient of 0.84. The results reveal distinct spatial patterns of water availability, with high ET values corresponding to irrigated and marshy areas, and low ET values in bare or sparsely vegetated zones. Despite limitations stemming from uncertainties in intermediate parameters, the proposed approach offers a robust and practical tool for regional-scale ET estimation in data-scarce environments. It supports informed decision-making in water resource management and enhances the operational monitoring of crop water needs.

Keywords: Actual evapotranspiration, Priestley–Taylor model, Landsat ETM+, Remote sensing, Triangle method, Water stress mapping, Semi-arid agriculture

INTRODUCTION

Monitoring the transfers of mass and energy at a surface is crucial for hydrological and vegetation resources management. It is also necessary for a better comprehension of hydrological and climatic systems. Remote sensing is an excellent tool for this monitoring as it provides information related to mass and energy transfers and particularly to evapotranspiration fluxes (Chibane and Ali-Rahmani, 2015; Hamimed et al., 2009; Hamimed et al., 2017; Soro et al., 2018).

Evapotranspiration is one of the fundamental processes controlling the equilibrium of our planet. It constitutes the link between the hydrological and energetic equilibrium at the soil-vegetation-atmosphere interface and its knowledge is crucial for climatic and agrometeorological studies. Depending on the geographical location on the earth's surface, evapotranspiration represents between 60 to 80 % of the precipitation return to the atmosphere (Brutsaert, 1982). Consequently, it constitutes one of major phenomena in the hydrological budget, especially in arid and semi-arid regions (Hamimed et al., 2014).

Furthermore, the estimation of actual evapotranspiration using satellite data in the visible and infrared has been at the centre of several methodological approaches during the last years. The deterministic models based, on more complex models such as Soil-Vegetation-Atmosphere Transfer models (SVAT) (Kalma et al., 2008), are mainly used for estimating evapotranspiration, surface energy exchanges and water balance. The following highly relevant papers provide strong examples of practical water-balance applications in semi-arid and karstic environments (Cherki, 2018; Qureshi et al., 2024).

Most of the transfer mechanisms, such as radiative, turbulent, and water transfers, as well as some physiological processes, such as photosynthesis, stomatal regulation are described. Their time resolution is less than one hour in agreement with the dynamic of atmospheric and surface processes. These models are however more cumbersome and use many parameters which are difficult to measure and make them unsuitable to spatial integration in models that are very sensitive to such parameters (Jacob, 1999).

From an operational point of view, we prefer using semi-empirical algorithms that express the convective flux through simple relationships. In most cases, these algorithms have been developed for determining instantaneous or daily evapotranspiration. The "simplified" semi-empirical relationship, proposed by Jackson et al. (1977), has allowed expressing the daily actual evapotranspiration based on the midday surface and air temperature difference (Seguin and Itier, 1983). The advantage of these relationships is to avoid three problems: 1) the estimation of the roughness length, involving in the sensible heat flux, 2) the lack of continuous measurement of surface temperature, and 3) the estimation of the soil heat flux which is negligible on daily timescales. However, it has limitations related to poor spatial representativeness of air temperature, measured locally, and the difficulty of taking into account the surface heterogeneity.

To take into account the fraction of vegetation cover in interpreting thermal infrared measurements, Gilles et al. (1997) proposed a so-called "Triangle method" in which they exploit the dimensions of a triangle resulting from the correlation between vegetation indices and surface temperature, highlighting the potential of this approach in estimating of evapotranspiration. A method using similar concepts, but a trapezoid rather than a triangle, was proposed by Moran et al. (1994).

Based on the existing links between the radiative and evaporative processes, i.e., albedo and surface temperature, used for the detection of water surfaces in extreme conditions, that is to say very dry and very wet, Roerink et al. (2000) proposed a very simple concept using no additional weather information, called S-SEBI (Simplified Surface Energy Balance Index) to estimate the evaporation fraction from the resolution of the balance equation energy for very dry and very wet surfaces.

Another possibility to estimate evapotranspiration is the use of so-called "residual" method, in which the latent heat flux is derived as the residual term of the energy balance equation (Kustas et al., 1994; Su, 2002). The implementation of these methods often requires additional information, such as weather, land use, vegetation height, etc… at time of satellite overpass.

The volition to use only information from remote sensing led Bastiaanssen et al. (1995) to develop an algorithm, called SEBAL (Surface Energy Balance Algorithm for Land) to solve the energy balance equation with a spatial approach assuming the existence of sites under extreme water conditions. The properties of these sites are used for determining some variables of the soil-plant-atmosphere interface not accessible with remote sensing, such as wind speed, the speed of thermal stability of the atmosphere, the resistance to turbulent transfer, and temperature air (Hamimed et al., 2008).

The overall intent of this study is to explore means for obtaining evapotranspiration maps for irrigated areas in Algeria, where ground data are scarce and hard to collect. A remote sensing approach is required to be routinely applied as a tool for providing both historical and near-real time evapotranspiration and surface energy fluxes for performing a better management of the agricultural water resources of the area. For this purpose, we use in this study data from Landsat ETM+ satellite to develop a methodology based on the triangle concept for accessing evapotranspiration through the classical expression of Priestley and Taylor (1972).

THEORETICAL BACKGROUNDS

Most remote sensing models or algorithms that have been developed for calculating actual evapotranspiration solve the surface energy balance. This latter describes the energy exchange between the land surface and the atmosphere, as follows:

$$Rn = G + H + \lambda E \tag{1}$$

where Rn is the net radiation at the surface, H is the sensible heat flux, *G* is the soil heat flux and λE is the latent heat flux (energy consumed by evapotranspiration). A key variable that plays a role in all these fluxes is the land surface temperature (T_o).

The net radiation is found from the various components of radiations exchanges, as follows:

$$Rn = \left(1 - r_o\right) Rg + L\downarrow - L\uparrow \tag{2}$$

where *Rg* is the incoming global radiation, partly reflected depending on the albedo r_o, L↓ and L↑ are the downwelling and the upwelling long wave radiations, respectively.

The soil heat flux *G* is usually low in comparison with the other terms. Therefore, we tend to neglect it, or to give it a fixed proportion of the net radiation (0.1 for example for bare soil). The sensible heat flux *H* is expressed as a function of the near-surface air temperature difference (T_o - T_a) as follows:

$$H = \frac{\rho Cp}{r_{ah}} (T_o - T_a) \tag{3}$$

where ρ is the air density, *Cp* is the air specific heat, T_o is the surface temperature, T_a is the air temperature and r_{ah} is the aerodynamic resistance to heat transport which is a function of wind velocity, thermal stability effects of the atmosphere and surface roughness. In satellite remote sensing applications, the land surface radiometric temperature (T_o) retrieval is often used instead of the aerodynamic temperature (T_{aero}) in Eq. (3).

To estimate the aerodynamic resistance to heat transport, some theoretical approaches have been used particularly by Paulson (1970) and are essentially based on the use of logarithmic profiles of mass and energy transfer in the surface boundary layer and the coupling between surface and boundary layer which occurs at the fluxes in the convective boundary layer. The integration of speed profiles leads to two similarity functions ψ_m and ψ_h parameterized by the turbulent regime of momentum and heat.

$$u^* = K\,u / \left[\ln(za / z_{om}) - \psi_m(za / L)\right] \tag{4}$$

$$r_{ah} = \frac{1}{K\ u^*}\left[\ln(za / z_{oh}) - \psi_h(za / L)\right] \tag{5}$$

where u is the wind speed at the reference height (usually 2 m), ψ_m and ψ_h are the momentum transport and heat transport stability corrections, respectively, *K* is the von Karman constant (≈ 0.41), z_{om} is the momentum transport roughness length and z_{oh} is the heat transport roughness length, u^* is the friction velocity, and *L* is the Monin-Obukhov's length expressed as:

$$L = -\frac{\rho Cp T_a u*^3}{K g H} \tag{6}$$

where g is the acceleration due to gravity.

The latent heat flux can be expressed as:

$$\lambda E = \frac{\rho Cp}{\gamma} \frac{e_{sat}(T_o) - e_a}{r_{ah} + r_s} \tag{7}$$

where γ is the psychrometric constant (Priestley and Taylor, 1972), r_s is the surface resistance to evaporation, e_a is the water vapour pressure at reference height za and $e_{sat}(T_o)$ is the saturated vapor pressure at surface temperature.

A practical way for estimating evapotranspiration from available data (meteorological data) by dispensing with surface temperature (generally difficult to measure) is by introducing the vapour pressure deficit in the air $\Delta e_{sat} = e_{sat}(T_a) - e_a$ into the difference $e_{sat}(T_o) - e_a$ (Penman, 1948; Monteith,1965):

$$e_{sat}(T_o) - e_a = \Delta(T_o - T_a) + \Delta e_{sat} \tag{8}$$

where Δ is the slope of saturated vapour pressure at the prevailing air temperature T_a. Combining Eqs. 1, 3, 7 and 8, can lead to the following expression of the Penman-Monteith latent heat flux (Monteith, 1965; Lagouarde et al., 1995; Guyot, 1999):

$$\lambda E = \frac{\Delta(Rn - G) + \rho Cp(\Delta e_{sat} / r_{ah})}{\Delta + \gamma(1 + r_s / r_{ah})} \tag{9}$$

This model is generally the most used to estimate directly potential evapotranspiration from meteorological measurements, by assuming r_s is zero. However, for actual evapotranspiration values, it has the disadvantage of being complicated, it requires knowledge of r_s and r_{ah} parameters difficult to estimate, which make it unsuitable for spatial integration in model that is very sensitive to such parameters (Hamimed, 2009).

Based on the fact that there is a strong correlation between ($Rn - G$) and Δe_{sat}, Priestley and Taylor (1972) proposed the following expression:

$$\lambda E = \alpha \frac{\Delta}{\Delta + \gamma}(Rn - G) \tag{10}$$

which represents the first term of the Penman-Monteith expression (Eq. 9) multiplied by an empirical dimensionless coefficient α called Priestley and Taylor parameter. This coefficient varies according to the surface type and is about 1.26 for wet land surface conditions (Kalma et al., 2008).

The Priestley and Taylor equation can be applied for unsaturated water surfaces provided adjusting α to each conditions type (Flint et al., 1991).

MATERIAL AND METHODS

The study area

The study area corresponds to the agricultural plain of Habra, which houses the irrigation area of Mohammadia. It is located in northwestern Algeria (Oran) between longitudes 0° 9' W and 0° 6' E and latitude 35° 34' N and 35° 43' N. It covers an area of 413 km^2 (Fig. 1).

The selected area is part of the great interior plain of Macta which is the receptacle of the second watershed of Algeria by its area (14,500 km²) and only communicates with the Mediterranean Sea by a narrow channel. The average altitude is about 40 m.

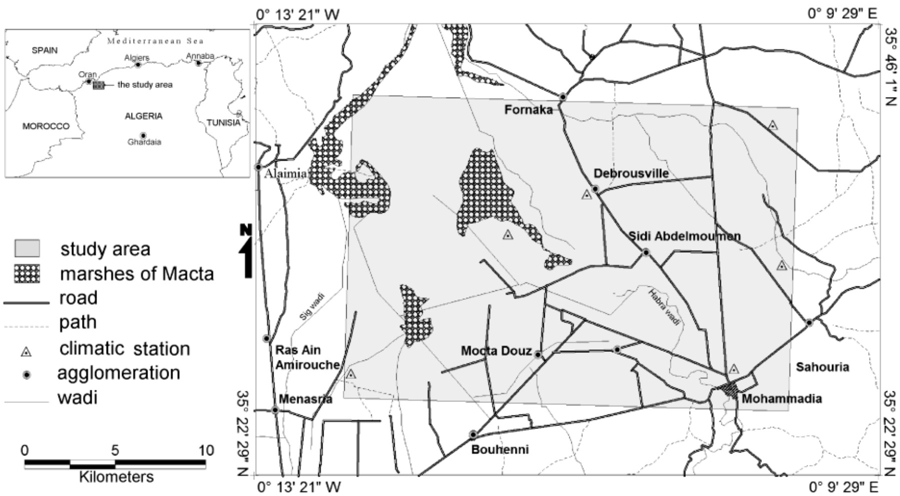

Figure 1: Map of the study area located in the Habra plain (Algeria)

The soils in the plain of Habra are sedimentary formation with variable texture intake alluvial and alluvio-colluvial. They are distributed in the plain into entities more or less uniform and regular. Soil salinity is between 8 and 16 mS.cm^{-1} at depth of more than 50 cm with low rate of leaching.

The climate in the study region is Mediterranean semi-arid with mild winter. Two main periods characterized this region, a rainy period during the months of autumn, winter and early spring and a dry and hot in summer. The absolute minimum air temperature during winter down to 6° C. Summer is usually dry and warm. The absolute maximum air temperature is equal to 42° C. The average annual rainfall for the period 1980-2005 is about 450 mm.

Fig. 2 shows the studied area Habra plain.

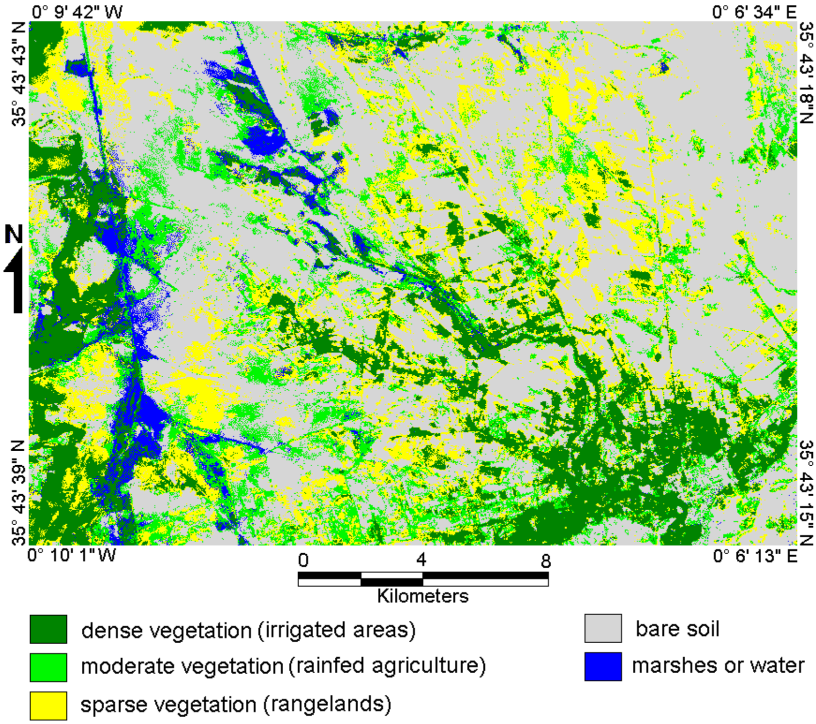

Figure 2: Land use map in the study area (Habra plain)

The rural areas with rich soils are suitable for agriculture but where the soils are poor, livestock grazing is dominant (Fig. 2). Irrigated agriculture is dominant in the study area and the main crops include fruits mainly citrus and garden crops such as artichoke. Rainfed agriculture occupies a small part and the main crops include cereals mainly barley. Water resources for irrigation are from Fergoug's dam located eight kilometres south of Mohammadia city.

REMOTE SENSING AND GROUND DATA

The data set used in this study consists of seven spectral bands of Landsat-7 ETM+ (Enhanced Thematic Mapper Plus) sensor acquired on May 29th, 2000 at 10 H 30' GMT. Optical bands (bands 1, 2, 3, 4, 5 and 7) were used for albedo and vegetation index calculations. Thermal band (band 6) was used for surface temperature. Spatial resolution is 30×30 m on the optical bands and 60×60 m on the thermal band. This high spatial resolution is well suited for monitoring evapotranspiration on heterogonous landscapes.

The spectral bands of ETM+ sensor are supplied in digit numbers (encoded into an 8-bit value) which are converted into radiances in the optical (visible, near and medium infrared) and thermal ranges using the linear relationship:

$$L_\lambda = A(DN) + B \quad (11)$$

where *DN* is the digit number and *A* and *B* are calibration coefficients.

The spectral radiances in the optical range are converted into reflectances after correction for atmospheric effects using MODTRAN radiative transfer code. These reflectances are then used to calculate the albedo (r_o) and vegetation index (NDVI). The albedo (r_o) is defined as a surface reflectance in the shortwave range (0.3-3 µm). It is calculated using the following formula:

$$r_o = 0.356\, r_1 + 0.13\, r_3 + 0.373\, r_4 + 0.085\, r_5 + 0.072\, r_7 - 0.0018 \quad (12)$$

where r_1, r_3, r_4, r_5 and r_7 are respectively the reflectances in channels 1, 3, 4, 5 and 7 of ETM + sensor. The vegetation index (NDVI) is calculated from the reflectances in the red (r_3) and the near infrared (r_4):

$$\text{NDVI} = \frac{r_4 - r_3}{r_4 + r_3} \quad (13)$$

The spectral space-reaching radiance measured by the sensor in the thermal infrared $L^{\uparrow}_{sat}$ (λ) is expressed by the following relationship:

$$L^{\uparrow}_{\text{sat}}(\lambda) = [\varepsilon_\lambda L_\lambda(T_o) + (1-\varepsilon_\lambda) L^{\downarrow}_{\text{atm}}(\lambda)]\, \tau_\lambda \; + L^{\uparrow}_{\text{atm}}(\lambda) \quad (14)$$

where $L_\lambda(T_o)$ is the radiance of a blackbody target of kinetic temperature T_o, τ_λ is the atmospheric transmission, $L^{\downarrow}_{\text{atm}}(\lambda)$ is the downwelling or sky radiance, $L^{\uparrow}_{\text{atm}}(\lambda)$ is the upwelling or atmospheric path radiance and ε_λ the emissivity of the surface which is estimated from the vegetation index (NDVI) (Van de griend et Owe, 1993):

$$\varepsilon_\lambda = 1.0094 + 0.047 \log(\text{NDVI}) \quad (15)$$

The atmospheric parameters are estimated at time of satellite overpass by the web atmospheric correction parameters calculator (Barsi et al., 2003). They allow deducing the spectral radiances leaving the land surface by inversion of Eq. (14). Surface temperatures are finally obtained based on these radiances according to Planck's Law:

$$T_o = \frac{1282.72}{\log\left[\dfrac{666.09}{L_\lambda(T_o)} + 1\right]} \quad (16)$$

Remote sensing data are supplemented by meteorological measurements for temperature and humidity of air, wind speed, global radiation, relative sunshine duration and daily evapotranspiration. These measurements are collected from six weather stations (Mohammadia, Debrousville, Sidi Abdemoumen, Sahouria, Menasria and Elghomri) located in the study area.

MODEL DESCRIPTION

The latent heat flux is estimated in pixel basis from the Priestley-Taylor expression [Eq. (10)], slightly modified by Flint et al. (1991) as follows:

$$\lambda E = \alpha_e \frac{\Delta}{\Delta + \gamma}(Rn - G) \tag{17}$$

which constitutes a generalization of the Priestley-Taylor expression in case of unsaturated water areas by introducing the α_e parameter that depends on the surface moisture and it ranges from 0 to 1.26.

The slope of saturated vapor pressure (Δ) is related to the air temperature (T_a) as (Allen et al., 1998):

$$\Delta = \frac{2503.058}{(T_a + 237.3)} exp\left(\frac{17.27 T_a}{T_a + 237.3}\right) \tag{18}$$

For estimating α_e in pixel basis, we propose an expression that combines the temperature vegetation dryness index (TVDI) (Sandholt et al., 2002) and the vegetation cover fraction (f_c) as follows:

$$\alpha_e = 1.26\left(1 - \mathrm{TVDI}\right) f_c \tag{19}$$

where f_c is expressed by Baret et al. (1995) as follows:

$$f_c = 1 - \left(\frac{\mathrm{NDVI}_{\max} - \mathrm{NDVI}}{\mathrm{NDVI}_{\max} - \mathrm{NDVI}_{\min}}\right)^{0.4631} \tag{20}$$

and the TVDI index is defined by the following relationship:

$$\mathrm{TVDI} = \frac{T_o - T_{o\,\min}}{T_{o\,\max} - T_{o\,\min}} \tag{21}$$

where $T_{o\,\min}$ and $T_{o\,\max}$ are respectively the minimum and maximum temperatures for a given NDVI value.

The TDVI index illustrates graphically the surface temperature as a function of NDVI. Its graphical space forms a triangle in which all combinations between NDVI and surface temperature are assumed shown (Fig. 3). The three points of the triangle, corresponding to the extreme surface conditions in terms of surface temperature and NDVI, allow deducting the extreme values $T_{o\ \min}$, $T_{o\ \max}$, $\mathrm{NDVI}_{\min}$ and $\mathrm{NDVI}_{\max}$ for the surface temperature and NDVI respectively (Jiang et Islam, 2001).

The other components of Eq. (17) are determined as follows. The estimation of net radiation (*Rn*) requires evaluation of the following:

- The incoming global radiation (*Rg*) obtained from exo-atmospheric solar radiation $K^{\downarrow}_{\mathrm{exo}}$ taking into account the transmissivity of atmosphere τ_{sw}:

$$Rg = K_{exo}{}^{\downarrow} \tau_{sw} \tag{22}$$

- The upwelling longwave radiation $L^{\uparrow}$ from Stephan-Boltzman law using surface temperature.

- The downwelling longwave radiation $L^{\downarrow}$ using air temperature and atmosphere emissivity (ε'). This latter is estimated following to (Brutsaert, 1975):

$$\varepsilon' = 1.24 \left(\frac{e_a}{T_\mathrm{a}} \right)^{1/7} \tag{23}$$

The soil heat flux *G* is empirically estimated using the following expression suggested by Bastiaanssen et al. (2000):

$$\frac{G}{Rn} = T_o \left(0.0038\, r_o + 0.0074\, r_\mathrm{o}^2 \right) \left(1 - 0.98\, \mathrm{NDVI}^4 \right) \tag{24}$$

involving albedo, vegetation index, surface temperature and net radiation.

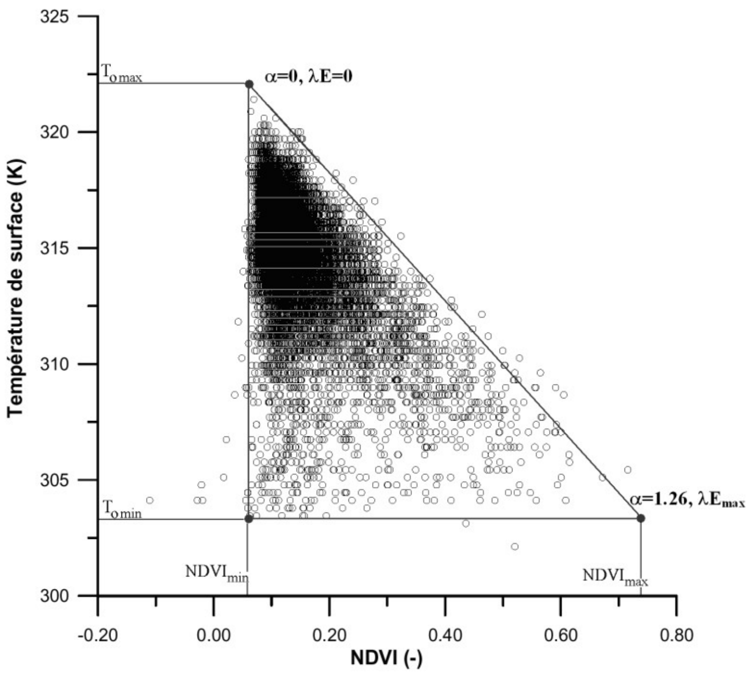

Figure 3: Plot of surface temperature versus normalized difference vegetation index (NDVI)

RESULTS AND DISCUSSION

Through modelling the different energy balance components, it has shown that the basic parameters albedo, vegetation index and surface temperature) obtained from the satellite imagery leads to determine the latent heat flux (λE) using the Priestley-Taylor expression.

The albedo was derived from a combination of reflectance in the short wavelength's bands. It varies for canopy on the image between 0.15 and 0.19, which seems acceptable.

The surface temperature was calculated from the radiance in the thermal infrared band using the vegetation index for estimating surface emissivity. An error of 1% on the emissivity value leads to an underestimation of the surface temperature of about 0.4-0.8 °C (Vidal et al., 1987). It would therefore be desirable to conduct advanced physical studies to increase the accuracy of the emissivity estimates. Indeed, surface temperature (T_o) is indirectly linked to the latent heat flux (λE) through the energy balance equation. It provides important information on surface water status. The analysis of correlation between T_o and λE shows a strong dependence between these two variables (r = 094). However, the NDVI and albedo, although they provide interesting information in interpretation of thermal data (Carlson, 2007; Menenti et al., 1989), are less significant in the discrimination of surface water status because their correlation coefficients with the latent heat flux are respectively 0.55 and 0.49.

The surface temperature varies on the image between 302.1 and 326.7 K. The higher values correspond to areas where bare soil are dominant, while low values are associated with areas where vegetation cover is dense. Similarly, the average surface temperature on dry pixels is higher than that on wet pixels.

The results presented in Table 1 summarize the energy fluxes and Priestley-Taylor parameter for different land use units. It was noted that high values of latent heat flux were observed on the irrigated areas with dense vegetation and water bodies, while low values are on the bare soils, corresponding to high values of albedo. This allows emphasizing that the spatial distribution of latent heat flux derived from the Priestley-Taylor expression is correlated to the water regimes of the different land use units.

In Fig. 4, actual evapotranspiration varies between 0 and 580W.m^{-2} with a clear dominance of surfaces subject to water stress more or less strong. However, the optimal water condition is only observed on a small area.

Another way to estimate the α_e parameter is based on the inversion of the latent heat flux derived from the SEBAL model (Khaldi et al., 2011). The comparison of the proposed approach and SEBAL model estimates of the α_e parameter shows good agreement (Fig. 5) which justifies the validity of the used approach.

Table 1: Variation of surface energy fluxes and the alpha parameter with land use in the study area

Land use units	***Rn*** (W.m^{-2})	***G*** (W.m^{-2})	α_e (-)	***λE*** (W.m^{-2})
Dense vegetation	720.1	155.6	1.12	329.9
Moderate vegetation	665.6	172.4	0.68	184.6
Sparse vegetation or bare soil	667.4	178.9	0.35	137.3
Marshes or open water	673.6	157.9	1.24	365.1

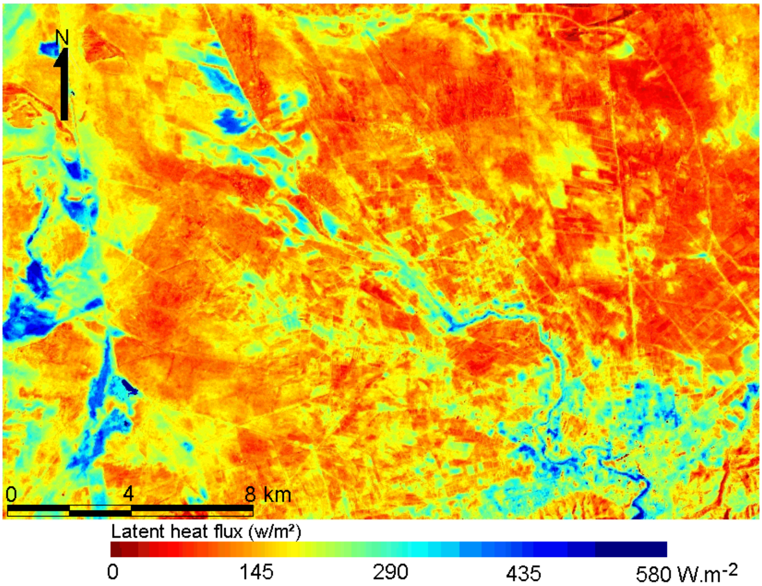

Figure 4: Latent heau flux map in the study area

Another method can be used for validating the obtained results. It is to compare latent heat flux values obtained from the proposed approach with those estimated on the ground using Bowen ratio. The result of this comparison is shown in Fig. 6. It shows a significant discrepancy between remote sensing and ground estimates of latent heat flux, with a RMSE about 49.6 W.m^{-2} and a correlation coefficient of 0.84, that was ascribed to inaccuracies on the intermediate variables such as surface albedo, emissivity, soil heat flux and air temperature.

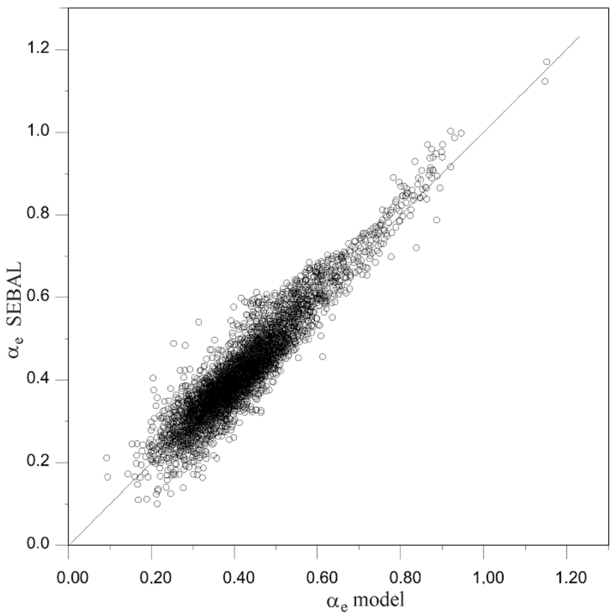

Figure 5: Comparison of the proposed approach and SEBAL model estimates of the α_e parameter

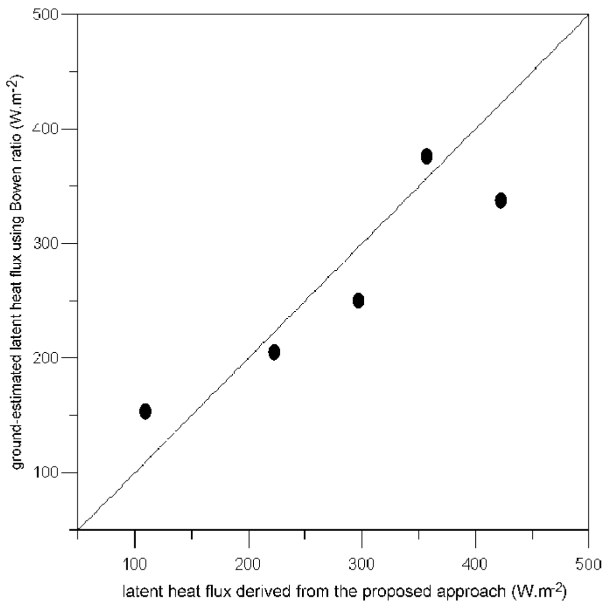

Figure 6: Comparison of ground-based and satellite-derived estimates of latent heat flux

CONCLUSION

This study has demonstrated the feasibility and effectiveness of integrating remote sensing data with a modified Priestley–Taylor model to estimate actual evapotranspiration (ET) over the semi-arid Habra Plain in northwestern Algeria. By employing the triangle method, which leverages the relationship between land surface temperature and vegetation indices derived from Landsat-7 ETM+ imagery, the spatial variability of the Priestley–Taylor coefficient (α) was captured with notable accuracy. This allowed for a realistic representation of water stress conditions across diverse land cover types and varying soil moisture regimes.

The validation of the model against ground-based Bowen ratio data and SEBAL estimates confirmed the reliability of the proposed approach, with a satisfactory correlation and acceptable error margins. The spatial maps generated provide valuable insights into water distribution, clearly delineating areas of agricultural irrigation, natural vegetation, and hydrologically stressed zones. These outputs are particularly relevant for water resource planning, irrigation scheduling, and monitoring of hydrological conditions in regions characterized by data scarcity and climatic constraints.

Despite certain limitations, such as uncertainties in atmospheric correction, parameter estimation, and model assumptions, the methodology proved operationally robust and adaptable to similar semi-arid environments. Future work could explore the integration of higher-resolution imagery and temporal datasets to refine ET dynamics over time. Overall, this work contributes meaningfully to the advancement of remote sensing applications in hydrological monitoring and underscores the vital role of evapotranspiration mapping in sustainable water management in arid and semi-arid regions.

REFERENCES

ALLEN R.G., PEREIRA L.S., RAES D., SMITH M. (1998). Crop evapotranspiration-guidelines for computing crop water requirements, Food and Agriculture Organization of the United Nations (FAO) irrigation and drainage Paper No 56, FAO, Roma, Italy, 300p., ISBN: 92-5-104219-5.

BARET F., CLEVERS J.G.P.W., STEVEN M.D. (1995). The robustness of canopy gap fraction estimates from red and near-infrared reflectances: a comparison of approaches, Remote Sensing of Environment, Vol. 54, Issue 2, pp. 141-151.

BARSI J.A., BARKER J.L., SCHOTT J.R. (2003). An atmospheric correction parameter calculator for a single thermal band earth-sensing instrument, IEEE International Geoscience and Remote Sensing Symposium (IGARSS'03), Proceedings, Vol. 5, pp. 3014-3016.

BASTIAANSSEN W.G.M. (1995). Regionalization of surface flux desities and moisture indicators in composite terrain: a remote sensing approach under clear skies in Mediterranean climates, Doctoral Thesis, Agricultural University of Wageningen (Landbouwuniversiteit Wageningen), The Netherlands, 271p.

BASTIAANSSEN W.G.M. (2000). SEBAL-based sensible and latent heat fluxes in the irrigated Gediz Basin, Turkey, Journal of hydrology, Vol. 229, Issue 1, pp. 87-100.

CARLSON T. (2007). An overview of the "triangle method" for estimating surface evapotranspiration and soil moisture from satellite imagery, Sensors, Vol. 7, Issue 8, pp. 1612-1629.

CHERKI K. (2018). Infiltration between GR5J modelling in the Oued N'Chef watershed and water balance calculation of Meffrouch dam (Tafna, northwest Algerian), Larhyss Journal, No 35, pp. 73-86

CHIBANE B., ALI-RAHMANI S.E. (2015). Hydrological based model to estimate groundwater recharge, real- evapotranspiration and runoff in semi-arid area, Larhyss Journal, No 23, pp. 231-242.

FLINT A.L., CHILDS S.W. (1991). Use of the Priestley-Taylor evaporation equation for soil water limited conditions in a small forest clearcut, Agricultural and Forest Meteorology, Vol. 56, Issue 3, pp. 247-260.

GILLIES R.R., KUSTAS W.P., HUMES K.S. (1997). A verification of the 'triangle method" for obtaining surface soil water content and energy fluxes from remote measurements of the Normalized Difference Vegetation Index (NDVI) and surface, International Journal of Remote Sensing, Vol. 18, Issue 15, pp. 3145-3166.

GUYOT G. (1997). Environmental Climatology, Masson Editions, Paris, France, 505p. (In French)

HAMIMED A., MENAA R., BENSLIMANE M., BOUABDELLAH L. (2008). Mapping of Daily Actual Evapotranspiration under Semi-Arid Conditions in Algeria Using ASTER Satellite Data, Science and Global Change/Sécheresse, Vol. 19, Issue 4, pp. 293-300. (In French)

HAMIMED A., KHALDI A., MEHOR M., SEDDINI A. (2009). Estimation of daily actual evapotranspiration in Algerian semiarid environment with satellite ASTER, EARSeL Proceedings, Vol. 8, Issue 2, pp. 140-151.

HAMIMED A., BENSLIMANE M., KHALDI A., NEHAL L., ZAAGANE M. (2014). Using the Priestley-Taylor expression for estimating actual evapotranspiration and monitoring water stress from satellite Landsat ETM + data, Larhyss Journal, No 18, pp. 179-195.

HAMIMED A., ZAAGANE M., OUALID A.T., TEFFAHI M., BAKHTIAR D. (2017). Monitoring daily actual evapotranspiration and surface water status over an agricultural area in western Algeria using remote sensing data, Larhyss Journal, No 29, pp. 45-59.

JACKSON R.D., REGINATO R.J., IDSO S.B. (1977). Wheat canopy temperature: a practical tool for evaluating water requirements, Water Resources Research, Vol. 13, Issue 3, pp. 651-656.

JACOB F. (1999). Use of Shortwave Remote Sensing and High-Resolution Thermal Infrared Imaging for the Estimation of Energy Fluxes at the Agricultural Plot Scale, Doctoral Thesis, Paul Sabatier University, Toulouse 3, France, (In French)

JIANG L., ISLAM S. (2001). Estimation of surface evaporation map over southern Great Plains using remote sensing data, Water Resources Research, Vol. 37, Issue 2, pp. 329-340.

KALMA J.D., McVICAR T.R., McCABE M.F. (2008). Estimating land surface evaporation: A review of methods using remotely sensed surface temperature data, Surveys in Geophysics, Vol. 29, Issues 4-5, pp. 421-469.

KHALDI A., HAMIMED A., MEDERBAL K., SEDDINI A. (2011). Obtaining evapotranspiration and surface energy fluxes with remotely sensed data to improve agricultural water management, African Journal of Food, Agriculture, Nutrition and Development, Vol. 11, Issue 1.

KUSTAS W.P., PERRY E.M., DORAISWAMY P.C., MORAN M.S. (1994). Using satellite remote sensing to extrapolate evapotranspiration estimates in time and space over a semiarid rangeland basin, Remote Sensing of Environment, Vol. 49, Issue 3, pp. 275-286.

LAGOUARDE J.P., OLIOSO A. (1995). Interest of mid-morning acquisition of surface temperature for deriving surface fluxes, Remote Sensing Reviews, Vol. 12, Issues 3-4, pp. 287-309.

MENENTI M., BASTIAANSSEN W., VAN EICK D., ABD EL KARIM M. A. (1989). Linear relationships between surface reflectance and temperature and their application to map actual evaporation of groundwater, Advances in Space Research, Vol. 9, Issue 1, pp. 165-176.

MONTEITH J.L. (1965). Evaporation and environment, In the Proceedings of the Symposia of the Society for Experimental Biology, Cambridge University Press (CUP), United Kingdom, UK, Vol. 19, No 205-23, pp. 205–234.

MORAN M.S., CLARKE T.R., INOUE Y., VIDAL A. (1994). Estimating crop water deficit using the relation between surface-air temperature and spectral vegetation index, Remote sensing of environment, Vol. 49, Issue 3, pp. 246-263.

PAULSON C.A. (1970). The mathematical representation of wind speed and temperature profiles in the unstable atmospheric surface layer, Journal of Applied Meteorology, Vol. 9, Issue 6, pp. 857-861.

PENMAN H.L. (1948). Natural evaporation from open water, bare soil and grass, Proceedings of the Royal Society of London, Series A, Mathematical and Physical Sciences, Vol. 193, Issue 1032, pp. 120-145.

PRIESTLEY C.H.B., TAYLOR R.J. (1972). On the assessment of surface heat flux and evaporation using large-scale parameters, Monthly Weather Review, Vol. 100, Issue 2, pp. 81-92.

QURESHI H.U., ABBAS I., SHAH S.M.H., TEO F.Y. (2024). Hydrologic evaluation of monthly and annual groundwater recharge dynamics for a sustainable groundwater resources management in Quetta city, Pakistan, Larhyss Journal, No 60, pp. 27-53.

ROERINK G.J., SU Z., MENENTI M. (2000). S-SEBI: a simple remote sensing algorithm to estimate the surface energy balance, Journal of Physics and Chemistry of the Earth, Part B: Hydrology, Oceans and Atmosphere, Vol. 25, Issue 2, pp. 147-157.

RUTSAERT W. (1975). On a derivable formula for long-wave radiation from clear skies, Water Resources research, Vol. 11, Issue 5, pp. 742-744.

SANDHOLT I., RASMUSSEN K., ANDERSEN J. (2002). A simple interpretation of the surface temperature/vegetation index space for assessment of surface moisture status, Remote Sensing of environment, Vol. 79, Issue 2, pp. 213-224.

SORO G.E., NOUFE D., GOULA BI T.A. (2018). Sensitivity analysis of a global hydrological model to the estimates of average rainfall and potential evapotranspiration: application to the Marahoue basin in Cote d'Ivoire, Larhyss Journal, No 23, pp. 115-168. (In French)

SU Z.B. (2002). On estimation of turbulent heat fluxes and evaporation with radiometric measurements: Past, Present and Future, Recent Advances in Quantitative Remote Sensing, In Sobrino J.A. Editions, Proceedings of the First International Symposium on Recent Advances in Quantitative Remote Sensing, University of Valencia, Valencia, Spain, 16-19 September, ISBN 84-370-5515-6, pp. 319–328.

TACONET O., BERNARD R., VIDAL-MADJAR D. (1986). Evapotranspiration over an agricultural region using a surface flux/temperature model based on NOAA-AVHRR data, Journal of Applied Meteorology, Vol. 25, pp. 284-307.

VAN DE GRIEND A.A., OWE M. (1993). On the relationship between thermal emissivity and the normalized difference vegetation index for natural surfaces, International Journal of remote sensing, Vol. 14, Issue 6, pp. 1119-1131.

VIDAL A., KERR Y., LAGOUARDE J.P., SEGUIN B. (1987). Remote Sensing and Water Balance: Combined Use of an Agrometeorological Model and Thermal Infrared Data from the NOAA-AVHRR Satellite, Agricultural and Forest Meteorology, Vol. 39, Issue 2, pp. 155-175. (In French)